

High Oxidation State Molybdenum Imido Heteroatom-Substituted Alkylidene Complexes

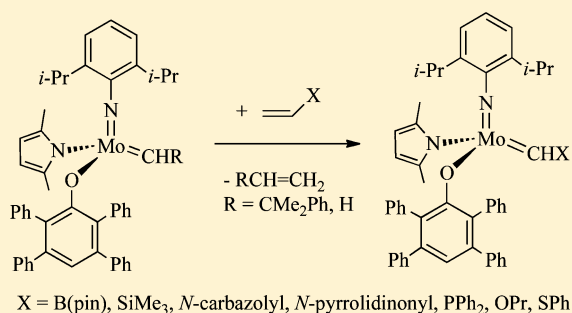
Erik M. Townsend,[†] Stefan M. Kilyanek,[†] Richard R. Schrock,^{*,†} Peter Müller,[†] Stacey J. Smith,[†] and Amir H. Hoveyda[‡]

[†]Department of Chemistry 6-331, Massachusetts Institute of Technology, Cambridge, Massachusetts 02139, United States

[‡]Department of Chemistry, Merkert Chemistry Center, Boston College, Chestnut Hill, Massachusetts 02467, United States

Supporting Information

ABSTRACT: Reactions between $\text{Mo}(\text{NAr})(\text{CHR})(\text{Me}_2\text{Pyr})(\text{OTPP})$ ($\text{Ar} = 2,6\text{-}i\text{-Pr}_2\text{C}_6\text{H}_3$, $\text{R} = \text{H}$ or CHCMe_2Ph , $\text{Me}_2\text{Pyr} = 2,5\text{-dimethylpyrrolide}$, $\text{OTPP} = \text{O-}2,3,5,6\text{-Ph}_4\text{C}_6\text{H}$) and $\text{CH}_2=\text{CHX}$ where $\text{X} = \text{B}(\text{pin})$, SiMe_3 , $N\text{-carbazolyl}$, $N\text{-pyrrolidinonyl}$, PPh_2 , OPr , or SPh lead to $\text{Mo}(\text{NAr})(\text{CHX})(\text{Me}_2\text{Pyr})(\text{OTPP})$ complexes in good yield. All have been characterized through X-ray studies (as an acetonitrile adduct in the case of $\text{X} = \text{PPh}_2$). The efficiencies of metathesis reactions initiated by $\text{Mo}(\text{NAr})(\text{CHX})(\text{Me}_2\text{Pyr})(\text{OTPP})$ complexes can be rationalized on the basis of steric factors; electronic differences imposed as a consequence of X being bound to the alkylidene carbon do not seem to play a major role. Side reactions that promote catalyst decomposition do not appear to be a serious limitation for $\text{Mo}=\text{CHX}$ species.



$\text{X} = \text{B}(\text{pin})$, SiMe_3 , $N\text{-carbazolyl}$, $N\text{-pyrrolidinonyl}$, PPh_2 , OPr , SPh

INTRODUCTION

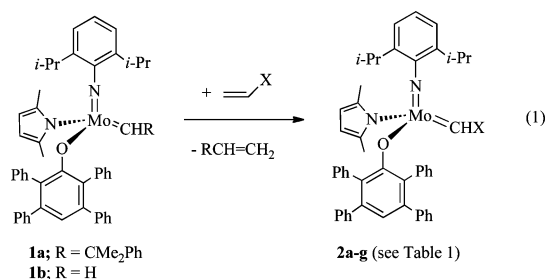
The vast majority of high oxidation state imido alkylidene complexes of Mo and W contain CHX alkylidenes in which X is carbon-based or, rarely, $\text{X} = \text{H}$.¹ A few $\text{M}=\text{CHX}$ complexes are known in which X is based on Si ¹ or Ge .^{1,2} However, to our knowledge no complexes have been described in which X is based on a heteroatom (B , N , O , S , P , halide, etc.). The only report of $\text{M}=\text{CHX}$ derivatives among high oxidation state alkylidene complexes concerns Re derivatives of the type $\text{Re}(\text{C-}t\text{-Bu})(\text{CHX})[\text{OCMe}(\text{CF}_3)_2](\text{THF})_2$ where X is OR , SR , or pyrrolidinonyl .³ In contrast, several $\text{Ru}=\text{CHX}$ derivatives have been described in which X is based on O , S , or N and for which selected reactions with olefins have been explored.^{4a} Also, several Ru -catalyzed metatheses involving enol ethers have been published.^{4b–c} As olefin metathesis investigations evolve to include $\text{CH}_2=\text{CHX}$ derivatives where X is not carbon-based (for example, Z -selective cross-metathesis reactions where $\text{X} = \text{OR}$ ⁵ or $\text{B}(\text{pinacolate})$ ⁶), it becomes more important to establish what Mo and W $\text{M}=\text{CHX}$ complexes can be prepared and how they react with ordinary olefins. Studies of high oxidation state $\text{M}=\text{CHX}$ compounds also would help clarify to what extent the electronic structure and reactivity of the $\text{Mo}=\text{C}$ bond are influenced by the presence of a heteroatom substituent.

RESULTS AND DISCUSSION

We targeted $\text{Mo}(\text{NAr})(\text{CHX})(\text{Me}_2\text{Pyr})(\text{OTPP})$ complexes ($\text{Ar} = 2,6\text{-}i\text{-Pr}_2\text{C}_6\text{H}_3$, $\text{Me}_2\text{Pyr} = 2,5\text{-dimethylpyrrolide}$, $\text{OTPP} = \text{O-}2,3,5,6\text{-Ph}_4\text{C}_6\text{H}$), in part because monoalkoxide pyrrolide (MAP) complexes have produced new and interesting results in

the last several years, especially Z -selective reactions,^{5–7} and because the OTPP ligand lowers the solubility and therefore facilitates isolation of what can otherwise be highly soluble MAP compounds. (An improved synthesis of 2,3,5,6-tetraphenylphenol (HOTPP) is described in the Supporting Information.)

In order to increase the simplicity of a reaction between a Mo alkylidene complex and $\text{CH}_2=\text{CHX}$ (eq 1), we prepared



$\text{Mo}(\text{NAr})(\text{CH}_2)(\text{Me}_2\text{Pyr})(\text{OTPP})$ (**1b**) in 79% yield, the Mo analogue of the tungsten complex, $\text{W}(\text{NAr})(\text{CH}_2)(\text{Me}_2\text{Pyr})(\text{OTPP})$,^{1c} by treating $\text{Mo}(\text{NAr})(\text{CHCMe}_2\text{Ph})(\text{Me}_2\text{Pyr})(\text{OTPP})$ (**1a**) with ethylene. The proton NMR spectrum of **1b** in C_6D_6 contains the methyldiene proton resonances at 11.77 and 11.58 ppm ($J_{\text{HH}} = 5$ Hz).

Both **1a** and **1b** react cleanly with $\text{CH}_2=\text{CHB}(\text{pin})$ to give $\text{Mo}(\text{NAr})[\text{CHB}(\text{pin})](\text{Me}_2\text{Pyr})(\text{OTPP})$ (**2a**), which is ob-

Received: June 20, 2013

tained as an orange solid in 83% yield. An X-ray study of **2a** (Figure 1) reveals that it contains an *anti* alkylidene ligand (i.e.,

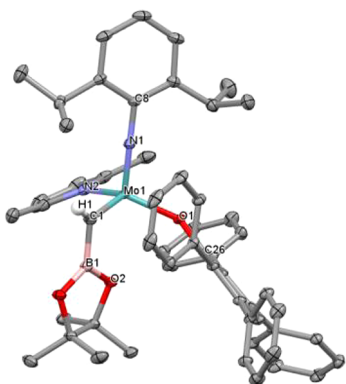


Figure 1. Thermal ellipsoid drawing of **2a** from XRD study.

the B(pin) substituent points away from the imido ligand) with a Mo=C bond length of 1.8825(1) Å and a Mo=C–B bond angle of 106.19(7)° (Table 1). These values should be

Table 1. Selected Mo=C Bond Lengths (Å) and Mo=C–X Bond Angles (deg) for Mo(NAr)(CHX)(Me₂Pyr)(OTPP) Complexes

cmpd	X	Mo=C	C–X	Mo=C–X
1a	CMe ₂ Ph ^a	1.881(5)	1.518(7)	145.2(4)
2a	B(pin) ^{b,c}	1.8825(1)	1.5525(16)	106.19(7)
2b	SiMe ₃	1.875(2)	1.862(1)	139.96(8)
2c	Carbaz ^d	1.9140(13)	1.3797(16)	143.60(10)
2d	Pyrrol ^{e,e}	1.9578(11)	1.3968(12)	117.47(7)
2e'	PPh ₂ ^f	1.904(2)	1.812(2)	126.1(1)
2f	OPr	1.921(3)	1.343(4)	142.7(3)
2g	SPh	1.9112(15)	1.7179(16)	130.20(9)

^aSee ref 6. ^bB(pin) = B(pinacolate). ^cAnti configuration. ^dCarbaz = N-carbazolyl. ^ePyrrol = N-pyrrolidinonyl. ^fAcetonitrile adduct.

compared with those for Mo(NAr)(CHCMe₂Ph)(Me₂Pyr)(OTPP) (**1a**, Table 1).⁶ NBO calculations reveal that the empty p orbital on B is conjugated with the Mo=C π orbital (Figure 2), but the contribution from the B orbital (99% p) is only 3.7% of the Mo=C π natural localized molecular orbital (NLMO). There is no evidence from either the NBO

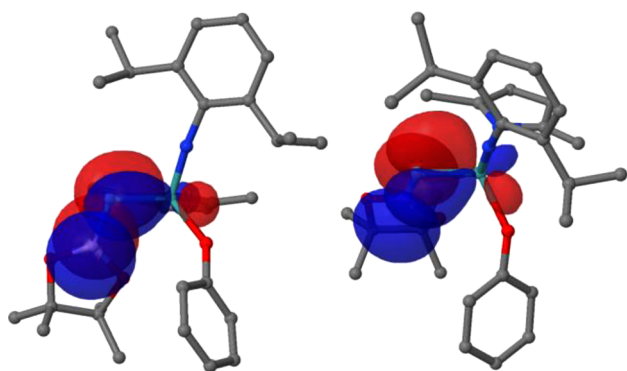


Figure 2. Overlap of the filled Mo=C π bond and the empty B p orbital in **2a** (preorthogonalized NBOs at the 0.02 isovalue). H atoms and OTTP phenyl rings have been omitted for clarity.

calculations or the Mo1...O2 distance (2.837 Å) that there is any significant electronic interaction between Mo1 and O2. A few structurally characterized 16e *anti* alkylidene complexes (i.e., five-coordinate intramolecular or intermolecular adducts) of this general type are known in which the M–C–C angle is 135–150°.^{1,10}

The proton NMR spectrum of **2a** (Figure 3) at 20 °C reveals broad alkylidene α proton resonances characteristic of

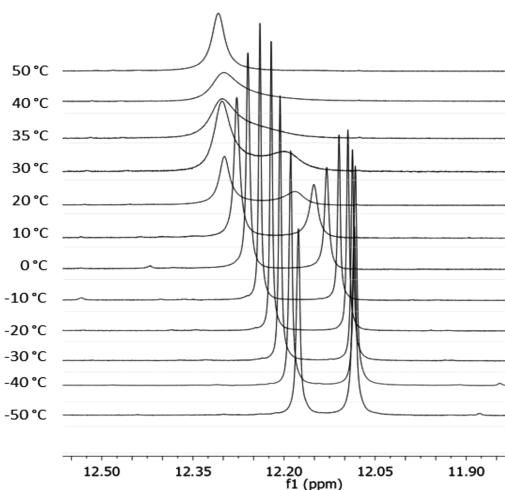


Figure 3. Temperature-dependent ¹H NMR spectra of **2a** in toluene-*d*₈ in the alkylidene proton region.

interconverting *syn* and *anti* isomers. Variable-temperature NMR studies (Figure 3) show one alkylidene resonance at high temperature and deconvolution and sharpening of two resonances at low temperature. Modeling the temperature dependence yields values of Δ*H*[‡] = 8.7(3) kcal/mol and Δ*S*[‡] = 0.02 kcal/(mol K); at 298 K the rate of interconversion is 28 s^{−1}. Therefore, both *syn* and *anti* isomers are accessible on a subsecond time scale in **2a** (at 298 K) and have approximately the same energies. The relatively high rate of alkylidene rotation is consistent with a Mo(+)–C=B(−) resonance form, although the π component of the Mo=C bond is only slightly decreased according to NBO calculations (*vide supra*).

The reaction between **1b** and CH₂=CHSiMe₃ yields Mo(NAr)(CHSiMe₃)(Me₂Pyr)(OTTP) (**2b**) as an orange solid in 47% yield. Compound **2b** is a single (*syn*) isomer in the solid state (see Table 1 and SI) and in solution (¹H NMR in C₆D₆). *Syn* and *anti* isomers of Mo(NAr)(CHSiMe₃)(OAr)₂ and W(NAr)(CHSiMe₃)(OAr)₂ have been observed in solution¹¹ and have been shown to interconvert readily at room temperature with a relatively low barrier (not quantified).¹² Since the amount of *anti* **2b** in solution is small, we cannot know whether *syn* and *anti* isomers of **2b** also interconvert readily.

The reaction between **1b** and CH₂=CH(Carbaz) (Carbaz = N-carbazolyl) yields Mo(NAr)[CH(Carbaz)](Me₂Pyr)(OTTP) (**2c**) as an orange solid in 81% yield. Compound **2c** is a single *syn* isomer in the solid state (see Table 1) and in solution (*J*_{CH} = 134 Hz; ¹H NMR in C₆D₆). The structure of **2c** (Figure 4) is consistent with previously characterized MAP complexes.

The reaction between **1b** and CH₂=CH(Pyrrol) (Pyrrol = N-pyrrolidinonyl) yields Mo(NAr)[CH(Pyrrol)](Me₂Pyr)(OTTP) (**2d**) as a pink solid in 81% yield. Compound **2d** is approximately a trigonal bipyramid (τ = 0.70)¹³ in which the

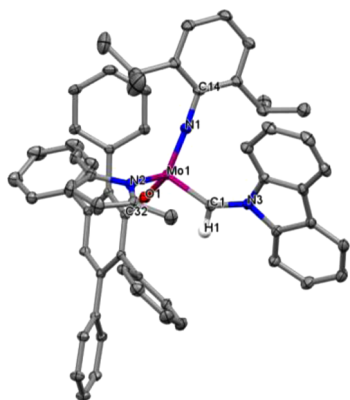


Figure 4. Thermal ellipsoid drawing of **2c** from XRD study.

carbonyl group is coordinated to the metal in an apical position (Figure 5). The alkylidene is *anti* with $J_{\text{CH}} = 166$ Hz; this

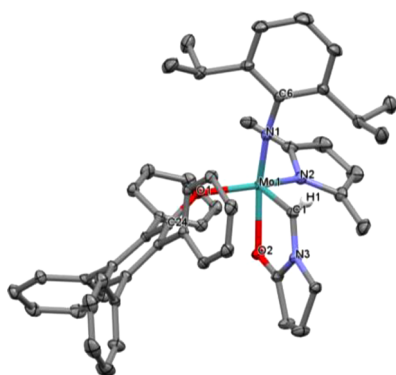


Figure 5. Thermal ellipsoid drawing of **2d** from XRD study.

configuration is expected on the basis of similar structures being observed for Re ($J_{\text{CH}} = 173$ Hz)³ and Ru⁴ complexes. The Mo=C bond distance in **2d** is longer than Mo=C bond distances in Table 1, probably as a consequence of the *anti* orientation of the alkylidene along with the fact that **2d** is five-coordinate. However, C=N multiple-bond character (and a consequent increase in the Mo=C bond length) is also suggested through NBO calculations.

The reaction between **1b** and $\text{CH}_2=\text{CHPh}_2$ yields $\text{Mo}(\text{NAr})(\text{CHPh}_2)(\text{Me}_2\text{Pyr})(\text{OTPP})$ (**2e**) as a red solid in 63% yield. Crystals were isolated as an orange acetonitrile adduct of **2e** (**2e'**) in 79% yield. The X-ray crystal structure of **2e'** is shown in Figure 6. Compound **2e'** is approximately a square pyramid ($\tau = 0.20$) with a *syn* orientation of the alkylidene in the apical position and an acetonitrile coordinated in a basal position *trans* to the pyrrolide. The Mo=C distance and Mo=C–P angle are normal, and the phosphorus is essentially pyramidal. NBO calculations reveal little to no contribution of the phosphorus lone pair to the Mo=C π bond, which is reasonable considering that the phosphorus lone pair is predominantly of *s* character and the reduced capacity of heavier main group elements to form multiple bonds to carbon.¹⁴ In solution, **2e** is a mixture of *syn* and *anti* isomers, as judged from its temperature-dependent proton NMR spectrum (Figure 7). The constant for coupling of the alkylidene proton to phosphorus in **2e** (the upfield resonance with $J_{\text{CH}} = 130$ Hz) is essentially zero, but approximately 5 Hz in the *anti* analog of

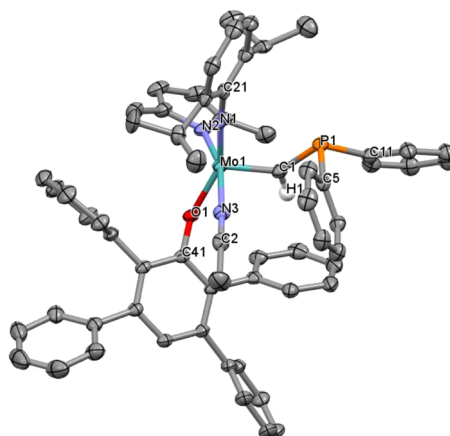


Figure 6. Thermal ellipsoid drawing of **2e'** from XRD study.

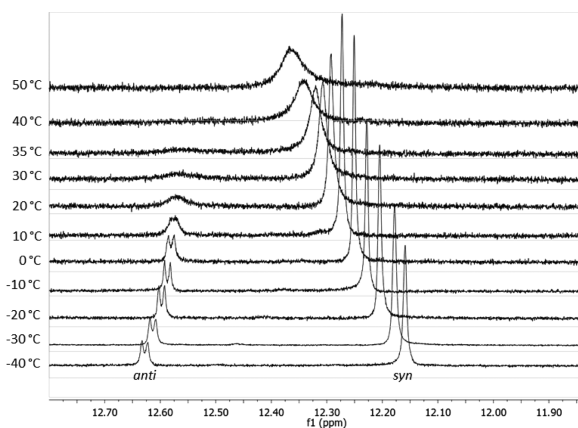


Figure 7. Temperature-dependent ^1H NMR spectra of **2e** in the alkylidene proton region in toluene- d_8 .

2e (the downfield doublet). Small (including zero)² J_{HP} values in general are not unusual.¹⁵

The ^1H NMR spectrum of **2e'** (in toluene- d_8 or C_6D_6 ; Figure 8) at 20 °C is virtually the same as the corresponding ^1H NMR spectrum of **2e** (Figure 7), consistent with acetonitrile not being bound strongly to the metal in solution at room temperature under these conditions. The temperature-depend-

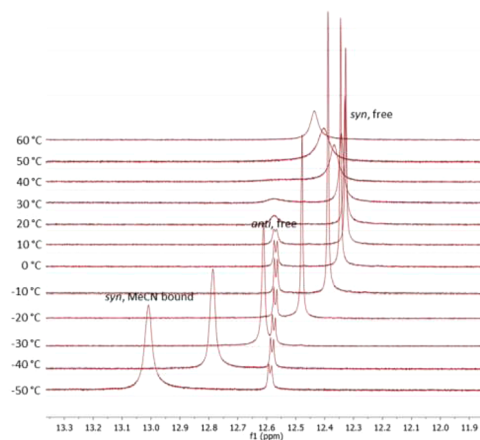


Figure 8. Temperature-dependent ^1H NMR spectra of **2e'** (13 mM in toluene- d_8) in the alkylidene proton region in the presence of ~ 1.5 equivalents of MeCN.

ent NMR spectrum of **2e'** in the presence of ~ 1.5 additional equivalents of MeCN (2.5 total MeCN per Mo) reveals similar coalescence behavior upon heating to the spectrum of **2e**. Upon cooling the sample, however, it appears that acetonitrile binds weakly to the *syn* isomer, as judged by a strong downfield shift of the *syn* alkylidene resonance at low temperatures (Figure 8). In contrast, the alkylidene proton of the *anti* isomer is relatively unaffected at low temperatures (Figure 8 versus Figure 7). We attribute lack of binding of acetonitrile to the *anti* isomer to donation of the phosphorus electron pair to the σ^* component of the Mo=N bond in *anti*-**2e**, which is the orbital that receives electron density in an agostic CH_α interaction in a typical *syn* alkylidene isomer.¹⁶

The reaction between **1a** or **1b** and $\text{CH}_2=\text{CHOPr}$ yields $\text{Mo}(\text{NAr})(\text{CHOPr})(\text{Me}_2\text{Pyr})(\text{OTPP})$ (**2f**) as an orange solid in 51% isolated yield. Its proton NMR spectrum at 22 °C shows a single alkylidene resonance with $J_{\text{CH}} = 140$ Hz, which should be compared with $J_{\text{CH}} = 135$ Hz for the *syn* isomer of $\text{Re}(\text{C}-t\text{-Bu})(\text{CHOEt})[\text{OCMe}(\text{CF}_3)_2](\text{THF})_2$ and 163 Hz for the *anti* isomer of $\text{Re}(\text{C}-t\text{-Bu})(\text{CHOEt})[\text{OCMe}(\text{CF}_3)_2](\text{THF})_2$ in solution.³ An X-ray study confirms that **2f** is a *syn* isomer in the solid state (Figure 9) with a Mo=C1 bond that is slightly

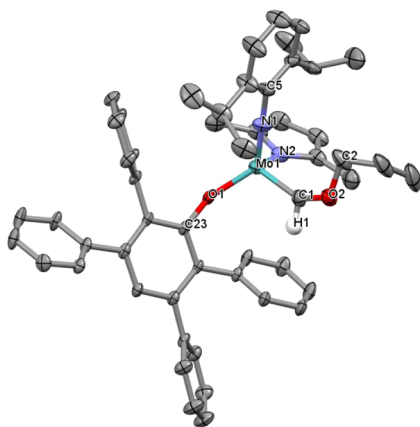


Figure 9. Thermal ellipsoid drawing of **2f** from XRD study.

elongated and a C1–O bond that is shortened (1.343(4) Å) compared to the C2–O bond length of 1.435(5) Å. NBO calculations reveal that the O lone pair donates electron density into the Mo=C π^* orbital (Figure 10). The NLMO of the lone pair contains a 7.0% contribution from the alkylidene carbon and a 3.4% contribution from Mo (98% d character).

The reaction between **1a** or **1b** and $\text{CH}_2=\text{CHSPh}$ yields $\text{Mo}(\text{NAr})(\text{CHSPh})(\text{Me}_2\text{Pyr})(\text{OTPP})$ (**2g**), which can be isolated as a red solid in 68% yield. Its proton NMR spectrum at 22 °C shows a single alkylidene resonance with $J_{\text{CH}} = 146$ Hz. An X-ray study shows that **2g** is the *syn* isomer in the solid state (Figure 11) with a Mo=C1 bond that is slightly elongated (1.9112(15) Å), a C1–S bond (1.7179(16) Å) that is shorter than the C2–S bond (1.7803(16) Å), and a C2–S–C2 bond angle of 105.99(8)°. The NLMO of the S lone pair contains a 5.1% contribution from the alkylidene carbon and a 4.7% contribution from Mo (98% d character).

In order to probe the competency of complexes **2a–g** as initiators for olefin metathesis reactions compared to **1a**, the conversion of 1-octene to *E/Z* 7-tetradecene by 5 mol % catalyst in C_6D_6 in a closed system (J-Young NMR tube) was monitored over time. The results are shown in Table 2. All reactions reach equilibrium ($\sim 50\%$ *E/Z* 7-tetradecene) in 0.5 h

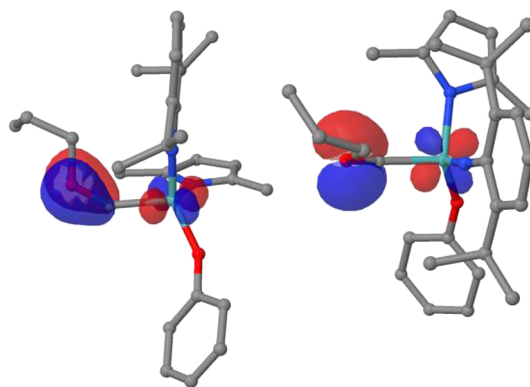


Figure 10. NLMO of the O lone pair (0.02 isovalue) showing an O lone pair overlapping with the Mo=C π^* antibonding orbital in **2f**. H atoms and the OTTPP phenyl rings have been omitted for clarity.

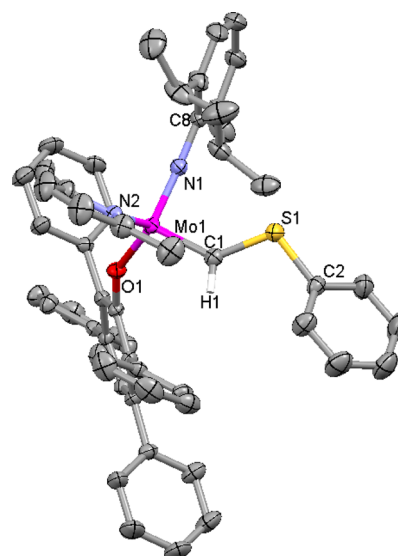


Figure 11. Thermal ellipsoid drawing of **2g** from XRD study.

Table 2. Percent Conversion for Metathesis Homocoupling of 1-Octene by **1a** and **2a–g** (5 mol %) in C_6D_6 at 22 °C (closed system)

	X	0.5 h	1 h	2 h	10 h
1a	CMe_2Ph	47	48	48	51
2a	B(pin)	47	47	47	49
2b	TMS	55	54	54	54
2c	Carbaz	50	50	50	53
2d	Pyrrol	0	0	3	12
2e	PPh_2	48	48	49	53
2f	OPr	47	47	47	49
2g	SPh	53	54	54	58

except the one involving **2d**. The slow initiation by **2d** is no surprise, given the relatively strong binding of the pyrrolidinone carbonyl group to the metal. In general, conversions are limited by equilibria that involve ethylene under the conditions employed.

In Table 3 are shown the relative amounts of the initial M=CHX complex and the heptylidene complex formed from it in the reactions between **1a** and **2a–g** and 20 equivalents of 1-octene. All except **2b**, **2d**, and **2g** form some observable and relatively constant amount of heptylidene ($\text{Mo}=\text{CHR}$) over a

Table 3. Ratios of $M=CHX$ to $M=CHR$ Complexes Observed in Reactions of **1a and **2a–g** with 1-Octene in C_6D_6 at 22 °C**

	X	0.5 h	2 h	10 h
1a	CMe ₂ Ph	0:100	0:100	0:100
2a	B(pin)	60:40	57:43	63:37
2b	TMS	100:0	100:0	100:0
2c	Carbaz	77:23	79:21	79:21
2d	Pyrrol	100:0	100:0	100:0
2e	PPh ₂	77:23	70:30	70:30
2f	OPr	13:87	14:86	15:85
2g	SPh	100:0	100:0	100:0

period of 10 h. Because **2b** and **2g** still carry out metathesis homocoupling rapidly (Table 2), we ascribe the lack of observable heptylidene to a thermodynamic preference for the $Mo=CHX$ species in each case. In the case of **2d**, the slow rate of homocoupling (*vide supra*) also suggests that the rate of initiation is slow.

Table 4 lists the percentage alkylidene remaining in reactions between $Mo=CHX$ complexes and 1-octene in C_6D_6 at 22 °C

Table 4. Percent Total Alkylidene Remaining in Reactions between $Mo=CHX$ Complexes and 1-Octene (15 equiv) in C_6D_6 at 22 °C as a Function of Time

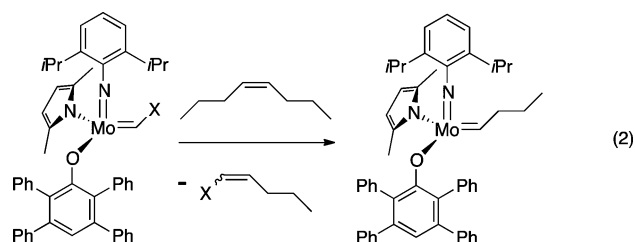
	X	0.5 h ^a	2 h	10 h	24 h
1a	CMe ₂ Ph	100	82	55	12
2a	B(pin)	100	100	66	18
2b	TMS	100	86	72	63
2c	Carbaz	100	91	68	37
2d	Pyrrol	100	100	100	100
2e	PPh ₂	100	92	34	0
2f	OPr	100	95	53	18
2g	SPh	100	92	60	36

^aInitial alkylidene present after 0.5 h is defined as 100%.

versus an internal standard as a function of time. All except **2d**, which is essentially inert, have decomposed to a significant degree after 24 h. In most cases decomposition is likely to involve bimolecular coupling of alkylidenes (especially methylenes) or rearrangement of metallacyclobutane complexes, including unsubstituted metallacycles.¹⁷

In order to investigate the relative reactivity of the heteroatom-substituted alkylidene complexes toward internal olefins, compounds **1a** and **2a–g** were treated with 15 equivalents of *cis*-4-octene in C_6D_6 and the disappearance of $Mo=CHX$ was monitored over time by ¹H NMR versus an internal standard. Complexes **1a**, **2b**, **2c**, **2d**, **2e**, and **2g** showed little to no conversion, even after 2 days. In contrast, **2a** and **2f** were rapidly converted to butylidene in a pseudo-first-order fashion.

A kinetic study of the rate of conversion to butylidene (eq 2) yielded first-order rate constants of $9.9 \times 10^{-5} M^{-1} s^{-1}$ for **2a** and $1.2 \times 10^{-3} M$ for **2f** (see SI for details). Compound **2f** reacts with *cis*-4-octene about 10 times faster than **2a** reacts with *cis*-4-octene, perhaps largely because the CHOPr ligand in **2f** is much smaller than the CHB(pin) ligand in **2a** near the metal. The relative rates of reaction of the *syn* or the *anti* isomers of **2a** are not known. Of the remaining unreactive species, **1a**, **2c**, and **2e** contain alkylidenes that are relatively sterically demanding. Finally, **2b**, **2d**, and **2g** show a strong



preference to remain in the $Mo=CHX$ form in the presence of terminal olefins (see Table 3), so the same should be true in the presence of an internal olefin.

CONCLUSIONS

Molybdenum and tungsten imido $M=CHX$ complexes in which X is based on B, Si, N, P, O, or S can be prepared readily. Rates of metathesis reactions can be rationalized on the basis of steric factors; electronic differences due to the presence of X bound to the alkylidene carbon do not seem to play a major role. However, the thermodynamic preference for catalyst resting state during a reaction depends on the nature of X. Side reactions do not appear to lead to a dramatic increase in rates of catalyst decomposition. Therefore, $Mo=CHX$ compounds could be intermediates in the known metathesis reactions that involve $Mo=CHX$ complexes in which X is based on O⁵ or B,⁶ and metathesis reactions that involve S- or P-based $Mo=CHX$ complexes should be possible. The data so far suggest that the presence of X on the alkylidene carbon does not dramatically alter the nature of the alkylidene and olefin metathesis reactions that involve them.

EXPERIMENTAL SECTION

Mo(NAr)(CH₂)(Me₂Pyr)(OTPP) (1b**).** A stir bar, 576 mg of **1a** (0.644 mmol, 1.0 equiv), and 30 mL of pentane were added to a 100 mL Schlenk bomb in a glovebox. (Compound **1a** did not completely dissolve.) The bomb was sealed, brought out of the box, and subjected to three freeze–pump–thaw cycles on a vacuum line. The solution was exposed to 1 atm ethylene and stirred for 3 h. The product precipitated as a light red powder. The bomb was brought into the glovebox, and the solid was filtered off and washed with cold pentane; yield 395 mg (79%). Anal. Calcd for C₄₉H₄₈MoN₂O: C, 75.76; H, 6.23; N, 3.61. Found: C, 75.59; H, 6.35; N, 3.55.

Mo(NAr)(CHBpin)(Me₂Pyr)(OTPP) (2a**).** In the glovebox, a 50 mL round-bottom flask was charged with a stir bar, 10 mL of toluene, 175 mg of **1b** (0.225 mmol, 1.0 equiv), and 57.3 μL of vinylboronic acid pinacol ester (0.338 mmol, 1.5 equiv). The flask was capped, and the contents were stirred for 3 h at room temperature. The solvent was removed *in vacuo*. Pentane (10 mL) was added, and the solvent was removed *in vacuo* again. Pentane (10 mL) was again added, and the red slurry was stirred and filtered to obtain 135 mg of pale orange product (66% yield). Compound **2a** can also be synthesized using the same procedure from Mo(NAr)(CHCMe₂Ph)(Me₂Pyr)(OTPP) and 2 equivalents of vinylboronic acid pinacol ester in 83% yield. Anal. Calcd for C₅₅H₅₉MoBN₂O₃: C, 73.17; H, 6.59; N, 3.10. Found: C, 72.82; H, 6.81; N, 2.93.

Mo(NAr)(CHSiMe₃)(Me₂Pyr)(OTPP) (2b**).** In the glovebox, a 50 mL round-bottom flask was charged with a stir bar, 10 mL of toluene, 166 mg of **1b** (0.214 mmol, 1.0 equiv), and 157 μL of trimethylvinylsilane (1.07 mmol, 5.0 equiv). The flask was capped, and the contents were stirred for 2 h at RT, after which time the solvent was removed *in vacuo*. Pentane was added (10 mL), and the solvent was removed *in vacuo* again. Pentane was again added (5 mL), and the red slurry was stirred and filtered to obtain 86 mg of pure orange solid product (47% yield). Anal. Calcd for C₅₂H₅₆MoN₂O₃Si: C, 73.56; H, 6.65; N, 3.30. Found: C, 73.24; H, 6.66; N, 3.21.

Mo(NAr)(CHCarbaz)(Me₂Pyr)(OTPP) (2c). In the glovebox, a 50 mL round-bottom flask was charged with a stir bar, 10 mL of toluene, 165 mg of **1b** (0.213 mmol, 1.0 equiv), and 41 mg of *N*-vinylcarbazole (0.213 mmol, 1.0 equiv). The flask was capped, and the contents were stirred for 4 h at RT. The solvent was removed *in vacuo*, pentane was added (10 mL), and the solvent was removed *in vacuo* again. Pentane was again added (10 mL), and the red slurry was filtered to obtain 163 mg of pure orange solid product (81% yield). Anal. Calcd for C₆₁H₅₃MoN₃O: C, 77.77; H, 5.88; N, 4.46. Found: C, 77.47; H, 6.15; N, 4.20.

Mo(NAr)(CHPyrrol)(Me₂Pyr)(OTPP) (2d). In the glovebox, a 50 mL round-bottom flask was charged with a stir bar, 10 mL of toluene, 200 mg of **1b** (0.257 mmol, 1.0 equiv), and 41 μL of *N*-vinylpyrrolidinone (0.386 mmol, 1.5 equiv). The flask was capped, and the contents were stirred for 4 h at RT. The solvents were removed *in vacuo*, pentane was added, and the solvent was removed *in vacuo* again. Pentane was again added, and the red slurry was filtered to obtain 171 mg of dark pink product (77% yield). Anal. Calcd for C₅₃H₅₃MoN₃O₂: C, 74.02; H, 6.21; N, 4.89. Found: C, 74.05; H, 6.28; N, 4.76.

Mo(NAr)(CHPPH₂)(Me₂Pyr)(OTPP) (2e) and MeCN Adduct (2e'). In the glovebox, a 50 mL round-bottom flask was charged with a stir bar, 8 mL of toluene, 119 mg of **1b** (0.153 mmol, 1.0 equiv), and 31 μL of diphenylvinylphosphine (0.153 mmol, 1.0 equiv). The flask was capped, and the contents were stirred for 3 h at RT, after which time the solvent was removed *in vacuo*. Pentane was added (10 mL), and the solvent was removed *in vacuo* again. Pentane was again added (10 mL), and the red slurry was stirred and filtered to obtain 92 mg of red product (63% yield). The acetonitrile adduct of **2e** can be obtained as an orange powder in 79% yield by adding acetonitrile in place of pentane in the workup. Compound **2e** appears to decompose slowly in the solid state, and **2e'** tended to lose acetonitrile. Therefore, consistent elemental analyses of either could not be obtained.

Mo(NAr)(CHOPr)(Me₂Pyr)(OTPP) (2f). In the glovebox, a 50 mL round-bottom flask was charged with a stir bar, 10 mL of toluene, 170 mg of **1a** (0.190 mmol, 1.0 equiv), and 43 μL of propyl vinyl ether (0.380 mmol, 2.0 equiv). The flask was closed, and the contents were stirred for 1 h at RT, after which time the solvent was removed *in vacuo*. Pentane was added (10 mL), and the solvent was removed *in vacuo* again. Pentane was again added (10 mL), and the red slurry was filtered to obtain 81 mg of orange product (51% yield). Anal. Calcd for C₅₂H₅₄MoN₂O₂: C, 74.80; H, 6.52; N, 3.36. Found: C, 74.88; H, 6.56; N, 3.36.

Mo(NAr)(CHSPh)(Me₂Pyr)(OTPP) (2g). In the glovebox, a 50 mL round-bottom flask was charged with a stir bar, 10 mL of toluene, 200 mg of **1a** (0.223 mmol, 1.0 equiv), and 58.3 μL of phenyl vinyl sulfide (0.446 mmol, 2.0 equiv). The flask was closed, and the contents were stirred for 19 h at RT, after which time the solvent was removed *in vacuo*. Pentane was added (10 mL), and the solvent was removed *in vacuo* again. Pentane was again added (10 mL), and the red slurry was filtered to obtain 133 mg of pink solid product (68% yield). Anal. Calcd for C₅₅H₅₂MoN₂OS: C, 74.64; H, 5.92; N, 3.17. Found: C, 74.46; H, 5.89; N, 2.99.

■ ASSOCIATED CONTENT

Supporting Information

General experimental details, NMR data for **1b** and **2a–g**, crystal parameters, data acquisition parameters, kinetic analyses, computational details, cif files, and a thermal ellipsoid drawing of **2b**. This material is available free of charge via the Internet at <http://pubs.acs.org>.

■ AUTHOR INFORMATION

Corresponding Author

*E-mail: rrs@mit.edu.

Notes

The authors declare no competing financial interest.

■ ACKNOWLEDGMENTS

We are grateful to the National Science Foundation (CHE-1111133 to R.R.S.) and to the National Institutes of Health (Grant GM-59426 to R.R.S. and A.H.H.) for financial support. We thank the National Science Foundation for departmental X-ray diffraction instrumentation (CHE-0946721).

■ REFERENCES

- (1) (a) Schrock, R. R. *Chem. Rev.* **2002**, *102*, 145. (b) Jiang, A. J.; Simpson, J. H.; Müller, P.; Schrock, R. R. *J. Am. Chem. Soc.* **2009**, *131*, 7770. (c) Schrock, R. R.; King, A. J.; Marinescu, S. C.; Simpson, J. H.; Müller, P. *Organometallics* **2010**, *29*, 5241. (d) Kreickmann, T.; Arndt, S.; Schrock, R. R.; Müller, P. *Organometallics* **2007**, *26*, 5702. (e) Peryshkov, D. V.; Schrock, R. R. *Organometallics* **2012**, *31*, 7278.
- (2) (a) Barinova, Y. P.; Bochkarev, A. L.; Begantsova, Y. E.; Bochkarev, L. N.; Kurskii, Y. A.; Fukin, G. K.; Cherkasov, A. V.; Abakumov, G. A. *Russ. J. Gen. Chem.* **2010**, *80*, 1945. (b) Barinova, Y. P.; Begantsova, Y. E.; Stolyarova, N. E.; Grigorieva, I. K.; Cherkasov, A. V.; Fukin, G. K.; Kurskii, Y. A.; Bochkarev, L. N.; Abakumov, G. A. *Inorg. Chim. Acta* **2012**, *363*, 2313. (c) Bochkarev, A. L.; Basova, G. V.; Grigorieva, I. K.; Stolyarova, N. E.; Malysheva, I. P.; Fukin, G. K.; Baranov, E. V.; Kurskii, Y. A.; Bochkarev, L. N.; Abakumov, G. A. *J. Organomet. Chem.* **2010**, *695*, 692. (d) Barinova, Y. P.; Bochkarev, A. L.; Kurskii, Y. A.; Abakumov, G. A. *Russ. J. Gen. Chem.* **2012**, *82*, 17.
- (3) Toreki, R.; Vaughan, G. A.; Schrock, R. R.; Davis, W. M. *J. Am. Chem. Soc.* **1993**, *115*, 127.
- (4) (a) Louie, J.; Grubbs, R. H. *Organometallics* **2002**, *21*, 2153. (b) Khan, R. K. M.; O'Brien, R. V.; Torker, S.; Li, B.; Hoveyda, A. H. *J. Am. Chem. Soc.* **2012**, *134*, 12774. (c) Katayama, H.; Urushima, H.; Nishioka, T.; Wada, C.; Nagao, M.; Ozawa, F. *Angew. Chem., Int. Ed.* **2000**, *39*, 4513. (d) Weeresakare, G. M.; Liu, Z.; Rainier, J. D. *Org. Lett.* **2004**, *6*, 1625. (e) Liu, Z.; Rainier, J. D. *Org. Lett.* **2005**, *7*, 131.
- (5) (a) Meek, S. J.; O'Brien, R. V.; Llaviera, J.; Schrock, R. R.; Hoveyda, A. H. *Nature* **2011**, *471*, 461. (b) Yu, M.; Ibrahim, I.; Hasegawa, M.; Schrock, R. R.; Hoveyda, A. H. *J. Am. Chem. Soc.* **2012**, *134*, 2788.
- (6) Kiesewetter, E. T.; O'Brien, R. V.; Yu, E. C.; Meek, S. J.; Schrock, R. R.; Hoveyda, A. H. *J. Am. Chem. Soc.* **2013**, *135*, 6026.
- (7) Wang, C.; Yu, M.; Kyle, A. F.; Jacubec, P.; Dixon, D. J.; Schrock, R. R.; Hoveyda, A. H. *Chem. Eur. J.* **2013**, *19*, 2726.
- (8) Wang, C.; Haefner, F.; Schrock, R. R.; Hoveyda, A. H. *Angew. Chem., Int. Ed.* **2013**, *52*, 1939.
- (9) Lee, Y.-J.; Schrock, R. R.; Hoveyda, A. H. *J. Am. Chem. Soc.* **2009**, *131*, 10652.
- (10) (a) Tonzetich, Z. J.; Jiang, A. J.; Schrock, R. R.; Müller, P. *Organometallics* **2006**, *25*, 4725. (b) Gerber, L. C. H.; Schrock, R. R.; Müller, P.; Takase, M. K. *J. Am. Chem. Soc.* **2011**, *133*, 18142.
- (11) Oskam, J. H.; Schrock, R. R. *J. Am. Chem. Soc.* **1993**, *115*, 11831.
- (12) (a) Schrock, R. R.; Murdzek, J. S.; Bazan, G. C.; Robbins, J.; DiMare, M.; O'Regan, M. *J. Am. Chem. Soc.* **1990**, *112*, 3875. (b) Schrock, R. R.; DePue, R. T.; Feldman, J.; Yap, K. B.; Yang, D. C.; Davis, W. M.; Park, L. Y.; DiMare, M.; Schofield, M.; Anhaus, J.; Walborsky, E.; Evitt, E.; Krüger, C.; Betz, P. *Organometallics* **1990**, *9*, 2262.
- (13) Addison, A. W.; Rao, T. J.; Reedijk, J.; van Rijn, J.; Verschoor, G. C. *J. Chem. Soc., Dalton Trans.* **1984**, 1349.
- (14) Epeotis, N. D.; Cherry, W. *J. Am. Chem. Soc.* **1976**, *98*, 4365.
- (15) Harris, R. K.; Woplin, J. R. *J. Magn. Reson.* **1972**, *7*, 291.
- (16) (a) Fox, H. H.; Schofield, M. H.; Schrock, R. R. *Organometallics* **1994**, *13*, 2804. (b) Poater, A.; Solans-Monfort, X.; Clot, E.; Copéret, C.; Eisenstein, O. *Dalton Trans.* **2006**, 3077.
- (17) Schrock, R. R. *Chem. Rev.* **2009**, *109*, 3211.